Applied Catalysis A: General 527 (2016) 137–145

Contents lists available at ScienceDirect

Applied Catalysis A: General

journal homepage: www.elsevier.com/locate/apcata

Synthesis of formaldehyde from dimethyl ether on alumina-supported molybdenum oxide catalyst

Raquel Peláez, Pablo Marín, Salvador Ordóñez*

Department of Chemical and Environmental Engineering, University of Oviedo, Faculty of Chemistry, Julián Clavería 8, 33006 Oviedo, Spain

ARTICLE INFO

Article history:
Received 29 May 2016
Received in revised form 2 September 2016
Accepted 7 September 2016
Available online 9 September 2016

Keywords:
Renewable chemicals
Biomass processing
Partial oxidation
Redox catalyst
Kinetic modelling

ABSTRACT

The selective oxidation of DME to formaldehyde over alumina-supported MoO_x catalyst (prepared by dry impregnation) is studied in this work. The activity and stability of the catalyst were evaluated in a fixed-bed continuous reactor at different temperatures and reactant concentrations.

The influence of the main operating conditions, (DME, O_2, CO_2 and CO feed concentrations; reaction temperature) on reaction rate and product selectivity was experimentally determined. Thus, DME conversion decreases on increasing DME feed concentration and increases on increasing O_2 feed concentration. Formaldehyde selectivity remained almost unaffected. A reaction mechanism, based on a Mars-van-Krevelen redox cycle representing DME oxidation to formaldehyde was used as a basis to develop a kinetic model for the reaction. The resulting simplified model suggests power law dependences for the reaction rate of 0.2 for the O_2 and 0.5 for the DME.

1. Introduction

The possibility of obtaining dimethyl ether (DME) from biomass with high yields has substantially increased the interest of this product as biofuel and a renewable chemical intermediate [1–4]. The process is based on the gasification of biomass into syngas, followed by syngas cleaning and its catalytic conversion into DME. In the traditional manufacture process of DME, the catalytic conversion of the syngas consists of two steps: the conversion to methanol and then the dehydration of methanol to DME [5].

Recent advances have shown that the direct synthesis of DME from syngas, where both reactions take place in the same reactor using bifunctional catalysts, is an attractive alternative. As an advantage, the thermodynamic limitations associated with the classical process are relaxed, leading to higher conversion and selectivity at lower pressure [1,6]. Thus, at the reaction conditions at which methanol synthesis process reaches only a 40% of CO conversion, DME synthesis from syngas can achieve more than 95% of CO conversion, with a high DME selectivity (67%) [7]. Therefore, DME production costs are largely lower, making this molecule into a competitive platform molecule.

Although DME can be used as alternative fuel, with limited soot formation when used in internal combustion engines [1,2], the synthesis of chemicals from DME is a very promising pathway in the chemical industry.

At this point, formaldehyde is a major product obtained by partial oxidation of methanol [8,9] (more than half amount of global methanol is used to produce formaldehyde [10]). The possibility of producing formaldehyde from DME would be a promising alternative route. In addition, several new generation fuels and fuel additives, such as 1,1,-dimetoxymethane and polyoxymethylene dimethylethers (POMMs), are synthetized from DME-formaldehyde mixtures [11].

A new alternative formaldehyde production method has emerged, after the new developments in the production of DME. Formaldehyde can be obtained by partial oxidation of DME over metal oxide catalysts. Several different catalysts have been proposed and tested for this reaction, but low reaction rates and selectivities have been reported. Mitsushima et al. proposed tungsten oxide (with or without additives) as catalyst, with a formaldehyde yield of 65–80%, although high temperatures, 673–773 K, are required [12]. Manganese nodules [13] are another material proposed in the literature for this reaction, but low formaldehyde yields were reported (<4%). The oxidation of DME over metallic silver catalysts yields a mixture of HCHO, alkanes, carbon oxides and water [14,15]. In addition, several authors suggest the use of mixtures of bismuth and molybdenum oxides with iron or copper oxides, or including with phosphorus and silicon [16,17]. These catalysts achieve values between 24 and 46% of conversion, with a formaldehyde selectivity of 14–45%, operating at

* Corresponding author.
E-mail address: sordonez@uniovi.es (S. Ordóñez).

http://dx.doi.org/10.1016/j.apcata.2016.09.002
0926-860X/

high temperatures (673–773 K). Some of these catalysts have significant yields but temperatures that are high are required and the oxidation of formaldehyde to carbon oxides was frequently reported, so it is necessary to propose alternative catalysts.

Recent studies of this reaction have proposed catalysts based on Mo and V oxides [18,19]. It has been reported that MoO_x and VO_x supported on Al_2O_3, ZrO_2 and SnO_2 present a good balance between reactivity and accessibility of oxide surfaces. The use of these materials has many advantages over other reported catalysts, mainly higher reaction rate and formaldehyde selectivity, together with a lower reaction temperature. In this sense, according to the reported results, MoO_x/Al_2O_3 is the most selective catalyst [18].

These studies suggest that the reaction proceeds via redox cycles where DME dissociation was followed by an oxidation using lattice oxygen. This is based on the fact that methanol oxidation to formaldehyde occurs via Mars-van-Krevelen redox cycles with surface methoxide intermediates and these intermediates can also be generated via C—O bond cleavage of the DME molecule [20–22].

Detailed kinetic studies have been developed for this reaction using zirconia-supported MoO_x catalysts [23]. For the alumina-supported MoO_x catalyst, several published studies report the reaction orders for DME and O_2 partial pressures [24,25].

Although alumina supported molybdenum oxide catalysts presented the best behavior, there are several aspects that have not been considered, such as the influence of carbon oxides on catalyst performance (typical components on DME feedstock derived from syngas), or the development of a more detailed kinetic model for this reaction with a MoO_3/Al_2O_3 catalyst.

The scope of this work is to fill these gaps providing the fundamental information necessary for design industrial processes for transforming DME into formaldehyde. To accomplish this goal, an alumina-supported MoO_x catalyst was prepared, characterized and tested in a fixed-bed continuous reactor. First, the stability of the catalyst upon time was studied. Then, a kinetic study was conducted varying the most important operating conditions (concentration of DME, O_2, CO and CO_2, and temperature). The experimental data was used for proposing a simplified kinetic model inspired on the mechanism proposed for the reaction.

2. Materials and methods

2.1. Chemicals and reactants

The reactant mixture consisted of dimethyl ether, O_2, CO, CO_2 and N_2 as balance gas. These reaction gases and chromatographic gases (He, H_2, Air) were supplied by Air Liquide with purities higher than 99%, and used without further purification.

2.2. Preparation of the MoO_x/Al_2O_3 catalyst

The catalyst was supported on γ-Al_2O_3 particles (BASF, surface area of 242 $m^2\,g^{-1}$), previously ground to 100–250 μm. The active phase was added by incipient wetness, using an aqueous solution of ammonium heptamolybdate tetrahydrate ($(NH_4)_6Mo_7O_{24}{\cdot}4H_2O$, 99% Fluka). The impregnated solid was dried at 373 K overnight and treated in an air flow at 775 K (10 K min^{-1} until 775 K, holding for 3 h) [10,18].

2.3. Catalyst characterization

The textural characteristics of the fresh and used catalysts were determined by nitrogen physisorption at 77 K in a Micromeritics ASAP 2020 analyzer by the Brunauer–Emmett–Teller (BET) method for the specific surface area, and the Barrett–Joyner–Halenda (BJH) approach to determine the pore volume and diameter.

The total amount of Mo on alumina was measured by Inductively Coupled Plasma Mass Spectrometer, ICP-MS, with collision cell (HP 7700, Agilent Technologies), after the total digestion of the sample in *aqua regia*.

The morphology of the catalytic material was investigated by Scanning Electron Microscope (SEM). The analysis was conducted using a JEOL-6610LV SEM-EDX. The samples were deposited on a standard aluminum holder and gold-coated. The metal surface concentration was also determined by EDX analysis.

X-Ray Diffraction (XRD) tests were carried out in a Seifert XRD 3000 diffractometer, which is equipped with a temperature controlled chamber.

Used catalysts were analyzed by Temperature-Programmed Oxidation (TPO) using a Micromeritics TPD/TPR 2900 coupled to a Pfeiffer Vacuum Omnistar Quadrupole Mass Spectrometer (MS). The samples were exposed to an oxidant gas (2% vol. O_2) while the temperature was increased (2.5 K min^{-1}) from 293 K to 1273 K. The evolution of CO and CO_2 concentrations was monitored continuously by MS. Temperature-programmed reduction (TPR) was also performed in the same device to determine the oxidation states of the catalyst, before and after the reaction. In the case, the samples were exposed to a reducing gas (10% vol. H_2 in Ar). The Origin Pro 8 analysis program was used for the signal processing.

The surface composition and binding energy of Mo, Al and C in the oxides were measured by X-ray Photoelectron Spectroscopy (XPS), using a SPECS system equipped with a Hemispherical Phoibos detector operating in a constant pass energy (Mg Kα radiation, $h{\cdot}\upsilon = 1253.6$ eV). During the deconvolution of the spectra, the full widths at half maximum of $Mo3d_{3/2}$ and $Mo3d_{5/2}$ were taken the same value, and the peak area ratio between both peaks was equal to 2:3. The full widths at half maximum of the C1s spectra for the different species were assumed to be equal, and this procedure was also applied for the O1s spectra.

2.4. Experimental device

Experiments were carried out in a continuous fixed-bed isothermal reactor. The reactor consisted of a stainless steel tube (9 mm diameter and 600 mm length) with the catalyst sample (2 g, 100–250 μm) placed inside. The catalyst was diluted with glass particles (6 g, 355–710 μm) in order to minimize temperature gradients within the catalyst bed. Temperature was measured by several thermocouples along the tube wall and one thermocouple placed inside the reactor tube. The latter was used to control the reactor temperature using a PID controller. The reactants were mixed at the desired proportions using different mass flow controllers (Bronkhorst High-Tech instruments).

The reactor effluent was maintained at 423 K using a heating tape to prevent formaldehyde condensation or oligomerization. On-line analysis of the reactor feed and effluent streams was carried out using a Gas Chromatograph (GC Agilent HP 6890N). It is equipped with a HP Plot Q capillary column for CO_2, DME, methanol, water and formaldehyde analysis, and a HP MoleSieve 5A capillary column for CO, O_2 and N_2 determination. The HP MoleSieve 5A column is connected to a valve which allows its connection or isolation from the system, according to the required analysis. Both columns are connected to two detectors: thermal conductivity (TCD) and flame ionization detectors (FID). The temperature program of the analysis is the following: 70 °C for 4.5 min, then a ramp of 10 °C/min up to 160 °C and a second ramp of 20 °C/min up to 200 °C and hold 5 min; finally, cold down to 70 °C at 30 °C/min and hold 11 min.

2.5. Reaction experiments

The catalyst stability was studied by operating the reactor at constant pass conditions for long reaction times (typically more

than 20 h). The influence of the different operating variables (e.g. temperature, DME, oxygen, CO and CO_2 concentrations) on catalyst performance was also studied.

DME conversion (X_{DME}) was calculated from the inlet and outlet DME molar fractions (y_{DME}) and the total molar flowrates (F) using the following expression:

$$X_{DME} = 1 - \frac{y_{DME}}{y_{DME feed}} \left(\frac{F}{F_0} \right) \quad (1)$$

The selectivity to the different products (S_i) was determined as the total amount of desired product formed per total amount of reactant consumed.

$$S_i = \frac{\left(y_i \left(\frac{F}{F_0} \right) - y_{i_{feed}} \right) / \nu_i}{\left(y_{DME_{feed}} X_{DME} \right) / \nu_{DME}} \quad (2)$$

where y_i and y_{ifeed} were the molar fraction of a compound in the outlet stream and in the feed respectively. F/F_0 corresponded to the ratio between the total molar flowrates in the outlet stream and in the feed, and it was obtained by applying the total molar balance to the reactor. The terms ν_i and ν_{DME} correspond to the stoichiometric coefficients of the compounds on the reaction, and X_{DME}, as already mentioned, is the DME conversion.

The error associated to the reaction experiments was estimated to be less than 5%.

The fixed-bed reactor has been modelled as plug-flow, according to the DME mass balance:

$$\frac{dX_{DME}}{d\bar{w}} = \frac{(-r_{DME})}{y_{DME_{feed}} SV} \quad (3)$$

Where $\bar{w}$ was the fractional length of the reactor fixed-bed (0 = inlet, 1 = outlet), $(-r_{DME})$ was DME reaction rate per unit weight of catalyst and $SV = F/W$ was the space velocity.

3. Results and discussion

3.1. Catalyst stability

The first studies were devoted to study the catalyst stability at reaction conditions in a continuous fixed-bed reactor. The reactor was operated at constant conditions, 0.2 MPa absolute pressure and 513 K, with a space velocity of 0.67 kmol kg^{-1} h^{-1} (feed flow rate of 0.5 NL min^{-1}). The feed composition was 10% DME and 13% O_2 with N_2 balance; hence, the reaction was carried out under oxygen-rich conditions. Reactor outlet concentrations were measured as a function of time to calculate conversion and selectivity.

The results indicated the existence of an initial stabilization period of 14 h, where DME conversion decreased as a function of time from 13% to 6% (Fig. 1). Afterwards, DME conversion was maintained constant. At this point, the main reaction products were formaldehyde, CO, methanol and CO_2, remaining the selectivity for formaldehyde formation higher than 65% during all the experiment. Concerning the other reaction products, selectivities for the formation of CO and CO_2 were always lower than 12 and 14%, respectively, whereas selectivity for methanol formation was about 8% during all the experiment. According to these facts, the reaction scheme depicted in Scheme 1 was proposed to describe the global process. In addition to DME oxidation to formaldehyde, side reactions of DME hydration to methanol and formaldehyde oxidations to form CO_x can take place. The possibility of CO oxidation to CO_2 over these catalysts, has been ruled out by additional experiments carried out with a CO feed at the same conditions.

A similar reaction scheme was reported in the literature [26] for formaldehyde synthesis from methanol, which resulted in the formation of dimethyl ether, methylal, methyl formate or carbon oxides, as secondary products. The formation of carbon oxides was due to a further oxidation of formaldehyde, with formic acid as intermediate (though rarely detected due to its low concentration).

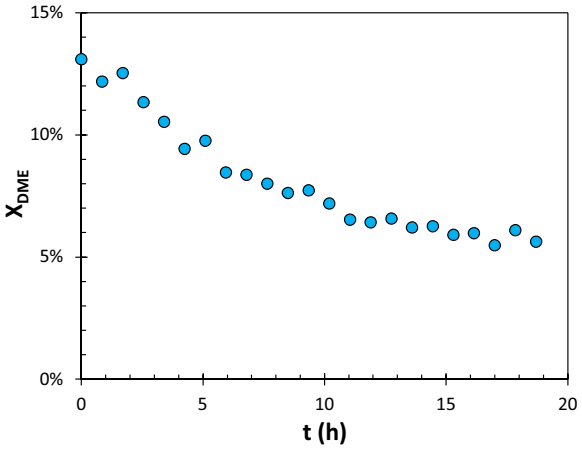

Fig. 1. Evolution of DME conversion with time on stream.

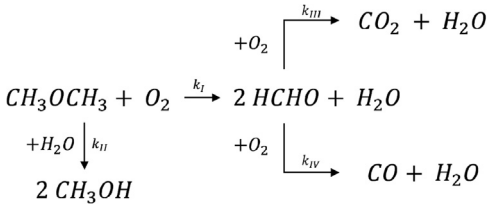

Scheme 1. Primary and secondary reaction pathways for dimethyl ether oxidation.

Table 1
Peak position in XPS spectra of MoO_3/Al_2O_3 system.

E_b (eV)	Mo $3d_{5/2}$	Mo $3d_{3/2}$	O1s	C1s
Fresh	233.3	236.5	531.2	284.6
				286.5
				288.8
Used	233.3	236.4	531.2	284.3
			533.5	286.8
				289.2

3.2. Catalyst characterization

Nitrogen physisorption analysis of the fresh and used catalysts showed a decrease in the surface area after reaction, from 230 to 144 m^2 g^{-1} (37% lower). This may explain the decrease in DME conversion during the catalyst stabilization. Fig. 2 shows the XPS spectra in the fresh and the used catalyst. The presence of two well resolved spectral lines, assigned to the $Mo3d_{5/2}$ and $Mo3d_{3/2}$ spin-orbit components were observed. The corresponding electron binding energies (E_b) are reported in Table 1. The experimental envelope of MoO_3/Al_2O_3 system was fitted to a single $Mo3d_{3/2}$–$Mo3d_{5/2}$ doublet (236.5 eV and 233.3 eV respectively). This indicates the presence of only one type of molybdenum (VI) oxo species, which strongly interacts with alumina surface. The XPS analysis conducted to the used catalyst presented the $Mo3d_{3/2}$–$Mo3d_{5/2}$ doublet at the same energies, suggesting that Mo oxidation state did not change after reaction.

These results are in good agreement with the reducibility of the surface species determined by TPR. Fig. 3 shows the TPR profiles of the MoO_x/Al_2O_3 catalyst before (a) and after (b) the reaction. Two main reduction regions were easily distinguished in both plots: at 533–733 K and 763–1193 K. The low temperature peak was attributed to a first reduction of Mo^{6+} to Mo^{4+} of octahedrally coor-

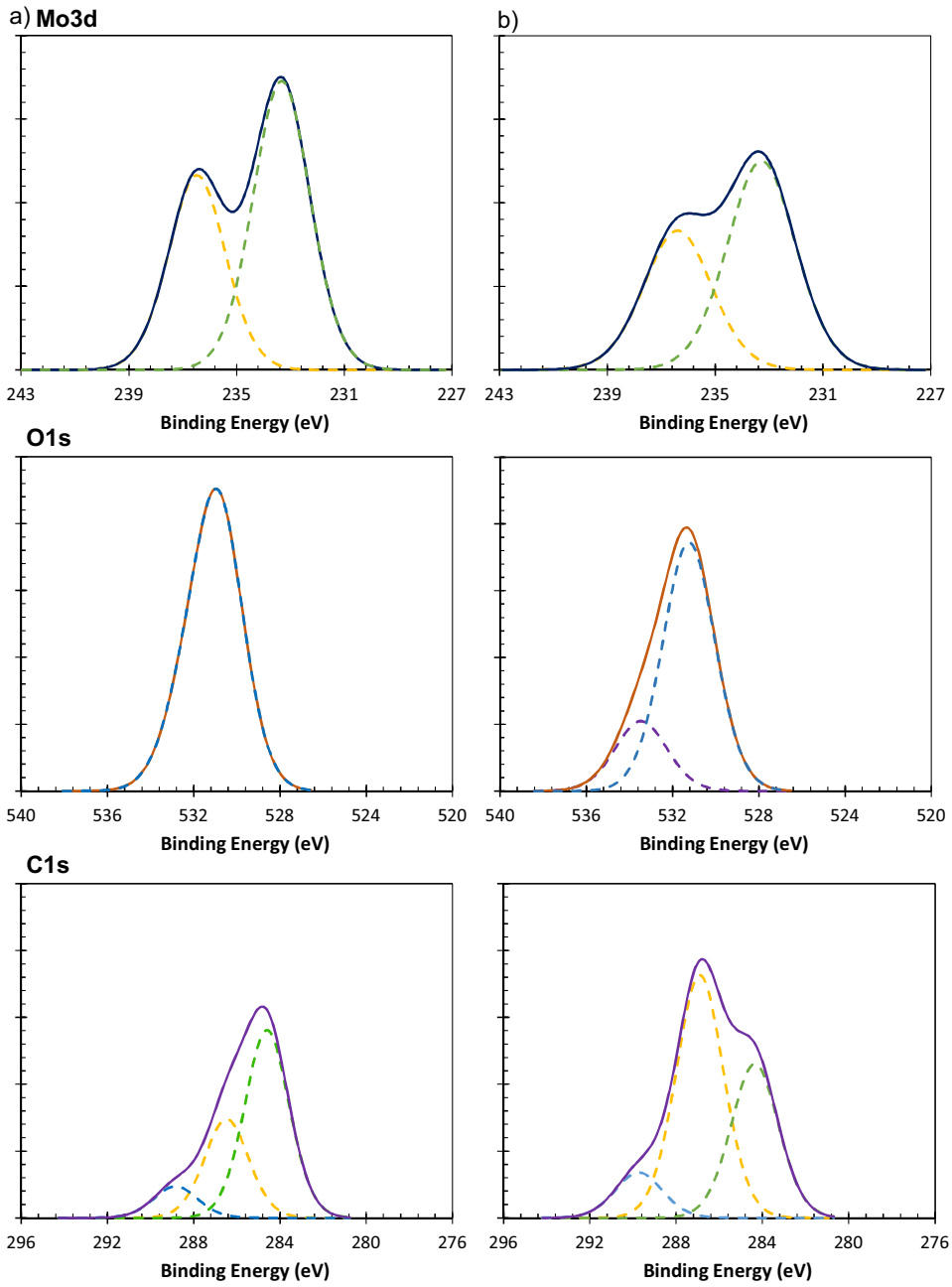

Fig. 2. XPS spectra of the fresh (a) and used (b) catalyst (Mo3d, O1s and C1s spectra).

dinated molybdenum species weakly bound to the support (Al_2O_3), predominantly as multilayer molybdenum domains, with some polymolybdates in monolayer patches [27]. The second reduction peak was associated to the reduction of Mo^{4+} to Mo^0 of molybdenum species strongly bound to Al_2O_3 and those previously partially reduced at low temperature [28]. Both reductions consumed a total amount of 1.6 mmol H_2 g_{cat}^{-1}, with a ratio between H_2 consumed in the two reduction peaks of 1/2 (0.54 mmol H_2 g_{cat}^{-1} in the first peak and 1.11 mmol H_2 g_{cat}^{-1} in the second). This is the stoichiometric relation between the Mo^{6+} and Mo^{4+} reduction reactions, so the reduction of Mo^{4+} in the second peak corresponds to the Mo^{6+} species previously reduced to Mo^{4+}. These findings confirm that only MoO_3 was present in the catalyst before and after the reaction.

The analysis of O1s and C1s XPS spectra provided new insights about the catalyst deactivation. The O1s spectra for the fresh catalyst showed a unique peak at binding energy of 531.2 eV. It is attributable to the overlapping of oxygen from MoO_3 and Al_2O_3, with energies of 230.6 eV and 231.1–231.4 eV [29]. Used catalyst O1s spectrum showed an additional peak at higher binding energy (533.5 eV). According to the reported results, peaks at ~530 eV was attributed to oxides whereas the peak at ~532 eV was due to organic oxygen species adsorbed on the catalyst surface [30]. This second analyzed peak can be assigned to methoxy species formed during the reaction, probably CH_3O-species bounded to multiple Mo ions [10]. This is confirmed by the C1s spectra. The C1s spectrum of the fresh catalyst corresponds with adventitious carbon, typically detected in samples that have been exposed to the atmosphere or generated during the analysis. By comparison with it, the C1s spectrum of the used catalyst shows higher amount of the component that appears at 286.8 eV. These binding energies have been reported to correspond to the methoxy species formed as reac-

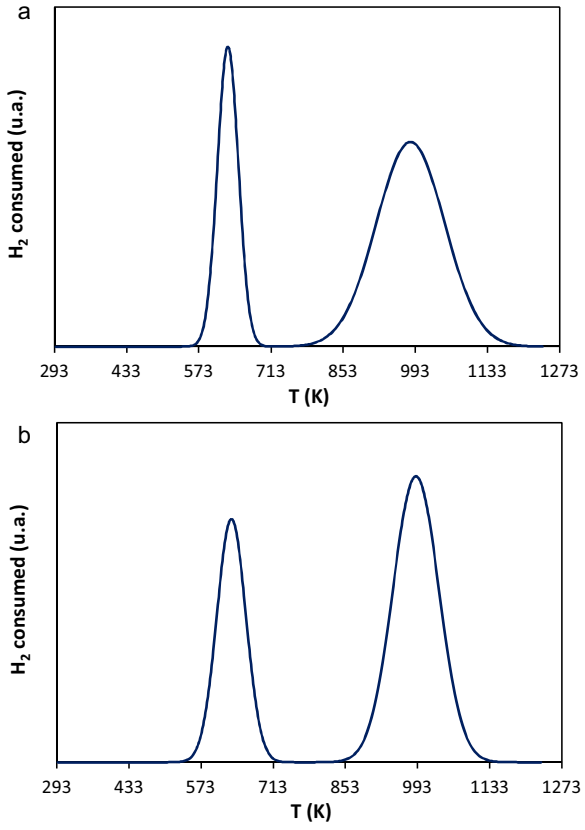

Fig. 3. TPR profiles for fresh (a) and used (b) catalyst.

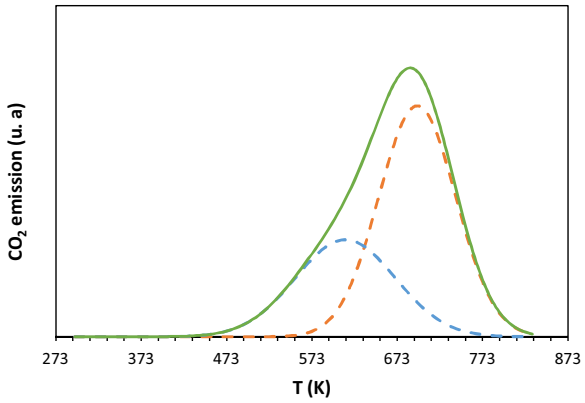

Fig. 4. TPO analysis of the catalyst after being used in the reaction.

tion intermediates and CO [10,31]. These methoxy species were probably bonded to more than two Mo ions and are related to CO_x formation [10]. A slight increase on the higher energy peak was also detected (289.2 eV). This peak can be attributed to CH_2O (288.8 eV), whose spectrum of oxygen (533.1 eV) could overlap with the corresponding to methoxy species [32].

The used catalyst was also analyzed by TPOs. The CO_2 release profiles were depicted in Fig. 4. The presence of a large peak in the range 573–773 K, with maximum at 697 K, indicates the presence of heavy organic compounds adsorbed on the surface of the catalyst that are oxidized at this temperature. The total amount of forming CO_2 on the aged catalyst corresponds with 188.3 μmol CO_2 g_{cat}^{-1}. The presence of these compounds is in agreement with the XPS measurements of the C1s spectrum (hydrocarbon and methoxy species).

Table 2
EDX analysis results of fresh and post-reaction catalysts.

% wt.	C	O	Al	Mo
Fresh	–	58.4	31.3	10.3
Std	–	6.3	5.3	1.3
Used	37.0	51.1	10.7	1.2
Std	2.9	1.7	1.8	0.09

The morphology and surface properties of the catalyst, obtained with a SEM-EDX, were compared before and after the reaction (Fig. 5). In fresh catalyst, it can be observed a uniform distribution of MoO_x particles on the surface the catalyst, suggesting an adequate preparation procedure. The elemental composition of the catalyst surface of the fresh and used catalysts was measured by EDX analysis in a 10–30 μm surface (Table 2). The results confirm the presence of C in the used catalyst, but also O was found in high amount. This fact suggested the formation of methoxy oligomers (with C and O) that can explain the decrease in conversion observed during the first 14 h in the catalyst stabilization test. After this time, the activity of the catalyst remained constant, suggesting that the formation of these species reached a steady state. The following kinetic tests have been carried out at steady state with the catalyst stabilization finished.

The X-ray diffraction patterns of the fresh catalyst did not show any reflections attributable to MoO_3, with only the presence of characteristic peaks of γ-Al_2O_3 being observed. At this point, Chen et al. [33] suggested the absence of Mo phases characteristic peaks for Mo surface densities lower than 5 Mo atoms nm^{-2}. It can be concluded that, as indicated by EDX analysis, the MoO_3 was well distributed on the support surface of the fresh catalyst, with a high dispersion. The chemical composition determined by ICP-MS analysis showed a total Mo concentration of 8.4% wt. on the catalyst

3.3. Kinetic experiments

The following reaction experiments were devoted to determine the kinetics of the DME oxidation reaction to formaldehyde. These experiments have been carried out during the constant activity period observed after 14 h of stabilization under reaction conditions.

The first set of experiments studied the influence of DME feed concentration within the range 3% to 14%. All the other operation conditions were kept unaltered: 13% O_2 (and N_2 balance), space velocity 0.94 kmol kg^{-1} h^{-1}, 2 bar and 518 K. Fig. 6 shows the results of the experiments in terms of DME conversion and product selectivity. DME conversion decreases from 17% to 7% when DME mole fraction in the feed increases from 3% to 14%. This fact suggests an apparent reaction order of DME much lower than one. On the contrary, the selectivity for the formation of different products remains almost constant. The main product obtained is HCHO with 69.0% selectivity, while the other products have a selectivity of: 20.6% for CO, 4.0% for CO_2 and 6.4% for methanol.

Typical DME feedstock derived from syngas is not composed only of DME, but can also contain other gases, such as CO and CO_2. The influence of these gases on the catalyst performance should be also considered. The effect of these gases on reactor performance was studied separately, by introducing reactor feeds with a 12% of CO_2 or 4% of CO, typical downstream concentrations in DME-containing streams derived from biomass. The rest components of the feed consisted of 10% DME and 13% O_2 (with N_2 balance). The operating conditions were the same as before: space velocity 0.94 kmol kg^{-1} h^{-1}, pressure 0.2 MPa and temperature 518 K. According to the experimental results, it can be concluded that both conversion and selectivity are not affected when a CO/CO_2-containing feed is introduced in the reactor.

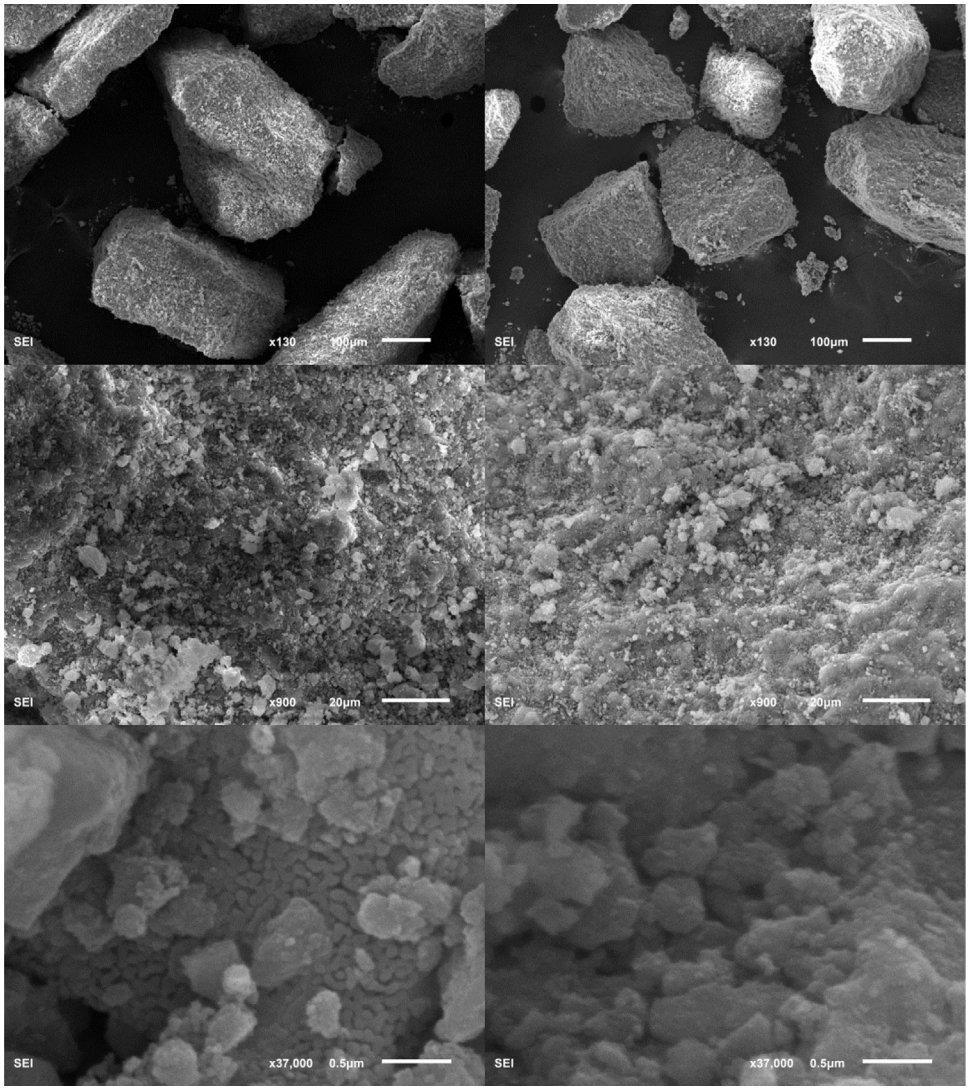

Fig. 5. SEM micrographs of fresh (a) and used (b) catalysts.

The influence of oxygen feed concentration was also assessed by means of experiments carried out in the range 1% to 13% O_2; with 10% of DME and N_2 balance, and the same operating conditions considered before. Fig. 7 shows that the influence of oxygen on DME conversion was more marked at low concentration; above 7% O_2, DME conversion was nearly constant to 9%. Regarding the selectivity of the different compounds, they were found to be constant also during this study.

The results of the kinetic experiments of this section have been fit to the following power-law empirical rate expression ($R^2 = 0.921$), using the plug flow reactor model of Eq. (3):

$$-r_{DME} = k[CH_3OCH_3]^{0.50}[O_2]^{0.20} \quad (4)$$

With $k = 8.73 \times 10^{-4}$ $mol^{0.3}\,(m^3)^{0.7}\,kg^{-1}\,s^{-1}$

This expression can be compared to the analogous one reported in the literature for methanol oxidation to formaldehyde [20]. The reported reaction order of methanol was close to unity, 0.94, which is almost double the value fitted for DME. This fact is explained considering the reaction mechanism described in the following section. Regarding oxygen, the reaction order was low, 0.10, but similar to the value obtained experimentally in the reaction studied in the present work.

Carberry number and Wheeler–Weisz criteria were applied in order to check the absence of external and internal mass transfer limitations for the most unfavorable conditions. To rule out internal and external heat transfer limitations determination, several parameters proposed in the literature were used [34].

The conditions at which external mass transfer is more likely to affect the overall kinetics correspond to a reactor feed of 14% DME, 13% O_2 (N_2 balance) at 518 K. For internal mass transfer, the worst conditions correspond to a reactor feed of 3% DME, 13% O_2 (N_2 balance) at the same temperature. The external mass transfer was discarded, with a Carberry number, $Ca = r_{obs}/K_G a_S C_G = 5 \times 10^{-6} < 0.05$, and the same was found with the internal mass transfer, Wheeler–Weisz criteria, $\eta\phi^2 = r_{obs} {d_p}^2/D_e C_S = 1 \times 10^{-1} < 0.1$. External heat transfer, $|\beta_{ex}\gamma^E Ca| = |K_G(-\Delta H)C_G E_a Ca/hRT_G{}^2| = 1 \times 10^{-3} < 0.05$, and internal heat transfer, $|\beta_{in}\gamma^E \eta\phi^2| = |D_e(-\Delta H)C_S E_a \eta\phi^2/k_e RT_S{}^2| = 9 \times 10^{-3} < 0.05$, were also negligible.

3.4. Reaction mechanism

The reaction mechanism shown in Table 3 is proposed to explain the oxidation of dimethyl ether to formaldehyde. This mechanism is based on previously reported studies [10,24] and the mechanism of methanol oxidation to formaldehyde proposed in the literature [20,26,35]. A new kinetic equation was developed and experimen-

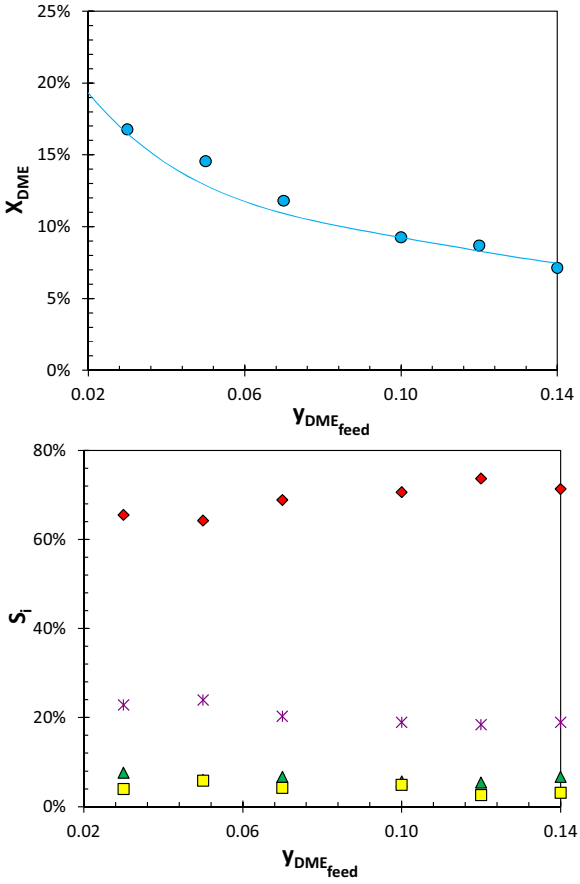

Fig. 6. DME feed concentration influence over (a) reactant conversion (●) and (b) selectivities to: formaldehyde (♦), methanol (▲), CO (✳) and CO_2 (■), in DME oxidation to formaldehyde (518 K, 2 bar, 21 $Nm^3\ kg^{-1}\ h^{-1}$).

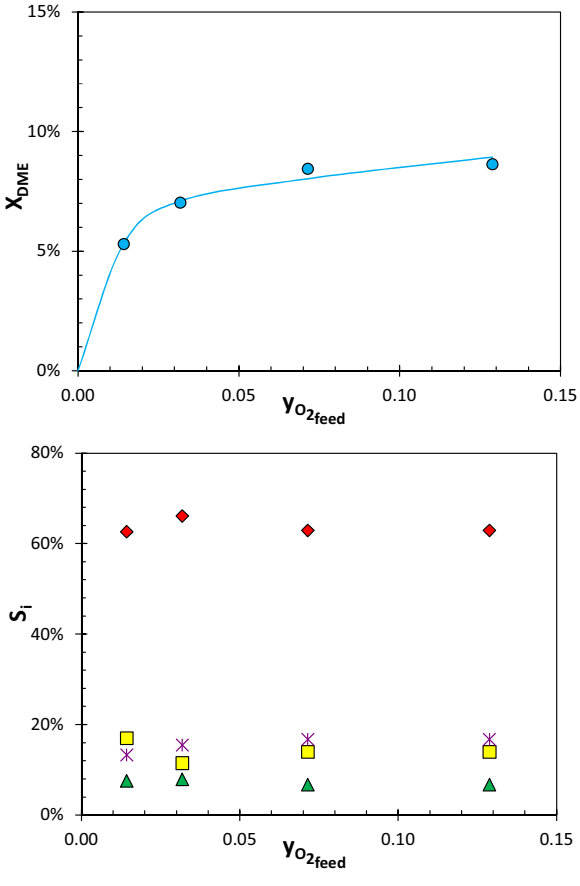

Fig. 7. Oxygen feed concentration influence over (a) reactant conversion (●) and (b) selectivities to: formaldehyde (♦), methanol (▲), CO (✳) and CO_2 (■), in DME oxidation to formaldehyde (518 K, 2 bar, 21 $Nm^3\ kg^{-1}\ h^{-1}$).

Table 3
Proposed mechanism for the oxidation of DME to formaldehyde catalyzed by MoO_x/Al_2O_3.

Adsorption	$CH_3OCH_3 + M^* + O^* \overset{K_1}{\leftrightarrow} M^* - O^* - CH_3OCH_3$
	$M^* - O^* - CH_3OCH_3 \overset{K_2}{\leftrightarrow} 2CH_3O^*$
Formaldehyde formation	$CH_3O^* + O^* \overset{k_3}{\rightarrow} HCHO + HO^* + *$
Methanol formation	$CH_3O^* + HO^* \overset{K_4}{\leftrightarrow} M^* + O^* + CH_3OH$
Water formation	$2HO^* \overset{K_5}{\leftrightarrow} M^* + O^* + H_2O$
Re-oxidation	$2* + O_2 \overset{K_6}{\leftrightarrow} 2O^*$

tally verified with the results of the kinetic experiments of the previous section.

The first step of the reaction pathway is the non-dissociative DME chemisorption, which occurs with interaction with lattice oxygen and metal sites. Then, the adsorbed DME dissociates yielding methoxide intermediates. Both steps are fast and assumed in equilibrium. Secondly, formaldehyde is generated by irreversible hydrogen loss of the methoxide species $*OCH_3$ promoted by a neighboring lattice oxygen atom. In this reaction, a *OH and a reduced Mo cation are also formed. Laterally, methanol production by $*OCH_3$ and *OH reversible reaction also can take place. Reversible reaction involving two *OH groups forms the water product of the reaction and the dissociative chemisorption of O_2 re-oxidizes the Mo sites.

According to the experimental results, the oxydehydrogenation of the methoxide $*OCH_3$ species to generate formaldehyde is the most likely rate-determining step of the mechanism. This mechanism is in agreement with that reported in the literature for the methanol oxidation mechanism, where the rate-determining step is the conversion of the methoxy intermediates to formaldehyde by abstraction of a hydrogen atom [20]. It is assumed that HCHO adsorption on the surface is weak, so it can desorb easily. Considering this reaction mechanism and the aforementioned assumption, the following kinetic expression was derived. The complete derivation is given as Supplementary information.

$$-r_{DME} = \frac{k_3/2(K_1K_2)^{1/2}C_t^2[CH_3OCH_3]^{1/2}}{\left(2 + (K_2K_1\,[CH_3OCH_3])^{1/2} + \left(\frac{1}{K_6[O_2]}\right)^{1/2}\right)^2} \quad (5)$$

3.5. Kinetic modelling

In this section, the proposed model was validated, and the parameters fitted, according to the results of the kinetic experiments.

- DME influence

In the experiments carried out varying the feed concentration of DME, O_2 was in excess, so its concentration can be assumed constant and the previous kinetic expression was simplified:

$$-r_{DME} = \frac{[CH_3OCH_3]^{1/2}}{\left(K' + K''[CH_3OCH_3]^{1/2}\right)^2} \quad (6)$$

This expression is only dependent on DME concentration. The parameters were fitted to the experimental data, considering the

fixed-bed as a plug flow, by the least-squares method using the EXCEL Solver. This has allowed us to determine that the term located in the denominator dependent of dimethyl ether concentration is not significant compared to those who accompany it, so the rate expression can be further simplified:

$$-r_{DME} = k_{apI}[CH_3OCH_3]^{1/2} \quad (7)$$

The adequacy of this last model was evaluated by comparison of experimental and predicted values, as shown in Fig. 6. The regression coefficient of the fit was $R^2 = 0.990$. It can be concluded that, in excess oxygen, the DME apparent reaction order proposed by the mechanistic kinetic model was in agreement with the experiments (0.5). According to the reaction mechanism, DME adsorbs and dissociates in two methoxide species $^*OCH_3$, which result in an apparent reaction order of 1/2. On the contrary, in the oxidation of methanol to formaldehyde, one methanol molecule generates only one methoxide, and for this reason the reaction order reported in the literature [20] was close to one.

- Oxygen influence

The findings of the previous section allowed the simplification of the general kinetic expression, Eq. (5):

$$-r_{DME} = \frac{k_3'[CH_3OCH_3]^{1/2}}{\left(1 + \frac{K_6'}{[O_2]^{1/2}}\right)^2} \quad (8)$$

The experiments performed at different oxygen feed concentrations were used to evaluate the validity of the denominator term regarding oxygen and fit the corresponding kinetic parameters. Fig. 7 shows the least-square fit of the model to the experimental data ($R^2 = 0.980$). The value of the model parameters is the following: the kinetic constant $k_3' = 1.51 \times 10^{-3}(m^3)^{0,5}(mol)^{0,5}\ kg^{-1}\ s^{-1}$ and O_2 adsorption constant $K_6' = 0.29\ mol^{0.5}/(m^3)^{0.5}$.

- Influence of the reaction temperature

The influence of temperature on the catalyst performance has been studied in the range 508–518 K, with a feed composed of 10% of DME and 13% of O_2 (N_2 balance). Fig. 8 shows the effect of this factor on DME conversion and product selectivity. On increasing temperature, conversion increased (from 5.0% at 508 K to 8.1% at 518 K), which was attributed to an increase in reaction rate. Formaldehyde was obtained as the major product at all temperatures, with a maximum selectivity of 70% reached at 515 K. This temperature corresponded to minimum selectivity towards CO (13.7%). On the contrary, the selectivity of both, methanol and CO_2 decreased with temperature.

The reaction was also tested at higher temperatures. However, when temperature was increased above 523 K, complete oxidation of formaldehyde was favored, which resulted in fast reaction and complete oxygen consumption. Therefore, the maximum recommended temperature for this reaction is 518 K.

The experiments were carried out in excess of oxygen, and also considering the findings of the previous sections regarding the kinetics of the reaction, the kinetic expression that can be used to describe the experiments at these conditions was Eq. (7). Using the conversion data, the apparent kinetic constant was calculated for each temperature, and fitted to the Arrhenius equation ($R^2 = 0.972$). The resulting activation energy was 108.5 kJ mol^{-1} and the pre-exponential factor $9.09 \times 10^7\ (mol)^{0,5}\ (m^3)^{0,5}\ kg^{-1}\ s^{-1}$. The activation energy of the analogous reaction of formaldehyde synthesis from methanol was, according to the literature, 98 ± 6 kJ mol^{-1} [20]. This value is slightly lower than the experimentally observed for formaldehyde synthesis from DME.

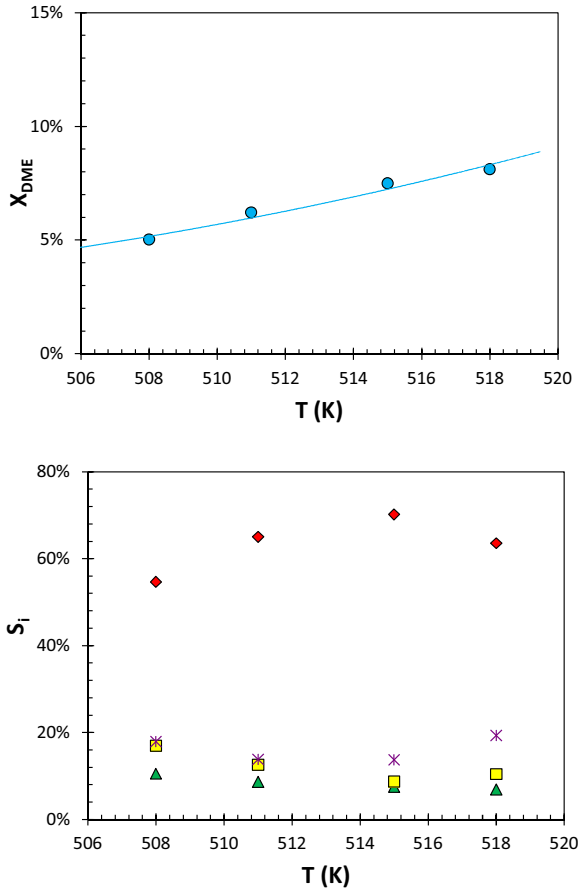

Fig. 8. Temperature effect over DME conversion (●) and selectivities to: formaldehyde (◆), methanol (▲), CO (✳) and CO_2 (■), in DME oxidation to formaldehyde (2 bar, 21 Nm^3 kg^{-1} h^{-1}).

Table 4
Summary of the main equations of the mathematical model proposed for the modelling of the oxidation of DME catalyzed by MoO_x/Al_2O_3.

Mass balance to the reactor	
$\frac{dF_{DME}}{d\tau} = -r_1 - r_2$	
$\frac{dF_{FAL}}{d\tau} = 2r_1 - r_3 - r_4$	$r_1 = k_{ap_I} C_{DME}^{1/2}$
$\frac{dF_{MeOH}}{d\tau} = 2r_2$	$r_2 = k_{ap_{II}} C_{DME}^{1/2}$
$\frac{dF_{CO_2}}{d\tau} = r_3$	$r_3 = k_{ap_{III}} C_{FAL}$
$\frac{dF_{CO}}{d\tau} = r_4$	$r_4 = k_{ap_{IV}} C_{FAL}$
$\frac{dF_{O_2}}{d\tau} = -r_1 - r_3 - \frac{1}{2}r_4$	
$\frac{dF_{H_2O}}{d\tau} = r_1 - r_2 + r_3 + r_4$	
Initial conditions	
$F_{DME\|_0} = F_{DME\|_{feed}}$	
$F_{FAL\|_0} = F_{MeOH\|_0} = F_{CO_2\|_0} = F_{CO\|_0} = F_{H_2O\|_0} = 0$	
$F_{O_{2\|_0}} = F_{O_{2\|_{feed}}}$	

3.6. Reaction model

Once the kinetic model corresponding to the reaction of DME oxidation to formaldehyde has been determined, the model was extended to all the reactions of Scheme 1. The compound balances and kinetic expressions are summarized in Table 4. By solving this model, both DME conversion and selectivity to formaldehyde can be predicted.

Table 5
Experimental values for the reaction apparent constants of the proposed reaction scheme at 518 K and 2 bar.

	$k_i \times 10^3$
k_I $[(m^3)^{0.5}(mol)^{0.5}\,kg^{-1}\,s^{-1}]$	1.04 ± 0.2
k_{II} $[(m^3)^{0.5}(mol)^{0.5}\,kg^{-1}\,s^{-1}]$	0.07 ± 0.1
k_{III} $[(m^3)\,kg^{-1}\,s^{-1}]$	0.60 ± 1.6
k_{IV} $[(m^3)\,kg^{-1}\,s^{-1}]$	3.02 ± 1.6

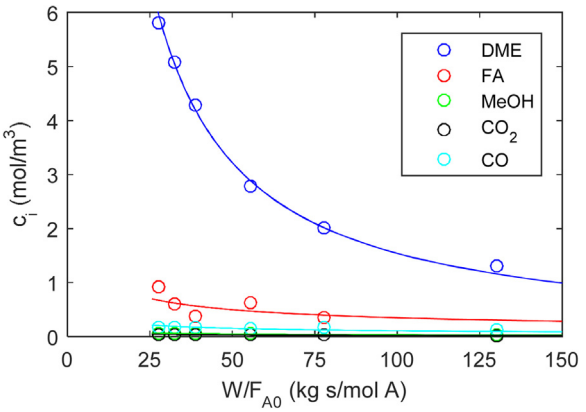

Fig. 9. Experimental data (○) and model prediction (—) to the study about the influence of DME initial concentration. DME (O), formaldehyde (O), methanol (O), CO_2 (○) and CO (O).

In order to get the model constants, the experimental data from the test performed at different initial DME concentrations were used. The model was solved in MATLAB using *ode15s*. The kinetic constants were fitted by the least square method using *lsqcurvefit*. Table 5 shows the obtained values and the corresponding confidence intervals. It can be observed that the reactions of synthesis of methanol and CO_2 did not have much significance in the overall reaction scheme, because the amount of these compounds was very low. Fig. 9 shows the experimental and model predicted concentrations of the different compounds. Formaldehyde was the main reaction product, being the oxidation of formaldehyde to CO the main side reaction.

4. Conclusions

The partial oxidation of dimethyl ether to formaldehyde was studied over a MoO_x/Al_2O_3 catalyst in an isothermal fixed-bed reactor. The use of this catalyst has been showed to be an efficient way of obtaining formaldehyde from DME. Although a slight deactivation was observed at the initial hours, mainly because of the formation of formaldehyde-derived oligomers, the catalyst reached steady state conditions. High (higher than 65%) and almost constant formaldehyde selectivity was obtained in the reported experiments.

Experimental results indicated that conversion depends on DME and O_2 concentration. A reaction mechanism based on the formation of methoxy intermediates, followed by the rate-limiting reaction over the oxidized catalyst centers, has been proposed. The kinetic model derived from this mechanism was found to represent the experimental data regarding dimethyl ether oxidation at different conditions.

The overall reaction scheme was also considered and the side reactions fitted to their corresponding kinetic models. Overall, formaldehyde formation was the most important reaction, followed by formaldehyde oxidation to carbon monoxide.

Acknowledgements

This work has been financed by Research Projects of the Regional Government of Asturias (project reference GRUPIN14-078) and Spanish Ministry of Economy and Competitiveness (CTQ2014-52956-C3-1-R) and by BPP company. Raquel Peláez acknowledges the Spanish Ministry of Education for the PhD grant that supports her research.

Appendix A. Supplementary data

Supplementary data associated with this article can be found, in the online version, at http://dx.doi.org/10.1016/j.apcata.2016.09.002.

References

[1] J. Sun, G. Yang, Y. Yoneyama, N. Tsubaki, ACS Catal. 4 (2014) 3346–3356.
[2] T.A. Semelsberger, R.L. Borup, H.L. Greene, J. Power Sources 156 (2006) 497–511.
[3] L. Faba, E. Díaz, S. Ordóñez, Renew. Sustain. Energy Rev. 51 (2015) 273–287.
[4] K. Takeishi, Y. Akaike, Appl. Catal. A: Gen. 510 (2016) 20–26.
[5] Z. Azizi, M. Rezaeimanesh, T. Tohidian, M.R. Rahimpour, Chem. Eng. Process. Process Intensif. 82 (2014) 150–172.
[6] V.V. Ordomsky, M. Cai, V. Sushkevich, S. Moldovan, O. Ersen, C. Lancelot, V. Valtchev, A.Y. Khodakov, Appl. Catal. A: Gen. 486 (2014) 266–275.
[7] J.L. Li, X.G. Zhang, T. Inui, Appl. Catal. A: Gen. 147 (1996) 23–33.
[8] R.E. Kirk, D.R. Othmer, Kirk–Othmer Encyclopedia of Chemical Technology, 4th ed., Wiley, New York, 1996.
[9] G. Reuss, W. Disteldorf, O. Grundler, A. Hilt, I.F. Ullmann, W. Gerhartz, Y.S. Yamamoto, F.T. Campbell, R. Pfefferkorn, J.F. Rounsaville (Eds.), Ullmann's Encyclopedia of Industrial Chemistry, 5th ed., Wiley-VCH, Deerfield Beach, FL, USA, 1985.
[10] X. Huang, J. Liu, J. Chen, Y. Xu, W. Shen, Catal. Lett. 108 (2006) 79–86.
[11] G.P. Hagen, M.J. Spangler, US Patent 6,160,186, BP Amoco Corporation (2000).
[12] H. Mitsushima, T. Murakami, H. Tadenuma, US Patent 3,655,771, Sumitomo Chemical CO. LTD (1972).
[13] R.M. Lewis, L.H. Slaugh, US Patent 4,435,602, Shell Oil Company (1984).
[14] G.P. Hagen, M.J. Spangler, US Patent 6,265,528, BP Corporation North America Inc (2001).
[15] L.B. Ralph, US Patent 2,246,569, The Solvay Process Company (1941).
[16] R.M. Lewis, R.C. Ryan, L.H. Slaugh, US Patent 4,439,624, Shell Oil Company (1984).
[17] R.M. Lewis, R.C. Ryan, L.H. Slaugh, US Patent 4,442,307, Shell Oil Company (1984).
[18] H. Liu, E. Iglesia, J. Catal. 208 (2002) 1–5.
[19] H. Liu, P. Cheung, E. Iglesia, Phys. Chem. Chem. Phys. 5 (2003) 3795–3800.
[20] W.L. Holstein, C.J. Machiels, J. Catal. 162 (1996) 118–124.
[21] S.T. Oyama, R. Radhakrishnan, M. Seman, J.N. Kondo, K. Domen, K. Asakura, J. Phys. Chem. B 107 (2003) 1845–1852.
[22] N. Pernicone, F. Lazzerin, G. Liberti, G. Lanzavecchia, J. Catal. 14 (1969) 293–302.
[23] H. Liu, P. Cheung, E. Iglesia, J. Phys. Chem. B 107 (2003) 4118–4127.
[24] P. Cheung, Liu, E. Iglesia, J. Phys. Chem. B 108 (2004) 18650–18658.
[25] X. Huang, Y. Li, Y. Xu, W. Shen, Catal. Lett. 97 (2004) 185–190.
[26] J.M. Tatibouët, Appl. Catal. A: Gen. 148 (1997) 213–252.
[27] V.M. Benitez, C.A. Querini, N.S. Fígoli, Appl. Catal. A: Gen. 252 (2003) 427–436.
[28] R. López Cordero, F.J. Gil Llambias, A. López Agudo, Applied Catalysis 74 (1991) 125–136.
[29] B.M. Reddy, B. Chowdhury, E.P. Reddy, A. Fernández, Appl. Catal. A: Gen. 213 (2001) 279–288.
[30] J.G. Choi, L.T. Thompson, Appl. Surf. Sci. 93 (1996) 143–149.
[31] O. Rodríguez de la Fuente, M. Borasio, P. Galletto, G. Rupprechter, H.J. Freund, Surf. Sci. 566–568 (Part 2) (2004) 740–745.
[32] C.T. Au, W. Hirsch, W. Hirschwald, Surf. Sci. 221 (1989) 113–130.
[33] K. Chen, S. Xie, A.T. Bell, E. Iglesia, J. Catal. 198 (2001) 232–242.
[34] J. Fernández, P. Marín, F.V. Díez, S. Ordóñez, Fuel Process. Technol. 133 (2015) 202–209.
[35] A.P.V. Soares, M.F. Portela, A. Kiennemann, Catal. Rev. 47 (2005) 125–174.